Control optimization of spherical modal liquid crystal lenses

A. F. Naumov and G. D. Love

Department of Physics and School of Engineering,

University of Durham, South Road, Durham, DH1 3LE, United Kingdom

g.d.love@durham.ac.uk

M. Yu. Loktev

P. N. Lebedev Physical Institute of Russian Academy of Science, Samara Branch,

221 Novo-Sadovaja St., 443011,Samara, Russia

F. L. Vladimirov

State Optical Institute, 12 Birjevaja linija, St.Petersburg, 199034, Russia

Abstract: Liquid crystal modal lenses are switchable lenses with a continuous phase variation across the lens. A critical issue for such lenses is the minimization of phase aberrations. In this paper we present results of a simulation of control signals that have a range of harmonics. Experimental results using optimal sinusoidal and rectangular voltages are presented. A lack of uniqueness in the specification of the control voltage parameters is explained. The influence of a variable duty cycle of the control voltage on an adaptive lens is investigated. Finally we present experimental results showing a liquid crystal lens varying its focal length.

OCIS codes: (010.1080) Adaptive Optics; (230.3720) Liquid-crystal devices.

References and links

1. V. Laude, "Twisted-nematic liquid-crystal pixelated active lens," Opt. Comm. **153**, 134-152 (1998).
2. W. W. Chan and S. T. Kowel, "Imaging performance of the liquid-crystal-adaptive lens with conductive ladder meshing," Appl. Opt. **36,** 8958-8969 (1997).
3. J. S. Patel and K. Rastani, "Electrically controlled polarization-independent liquid-crystal Fresnel lens arrays," Opt. Lett. **16**, 532-534 (1991).
4. C. W. Fowler and E. S. Pateras, "Liquid crystal lens review," Ophthal. Physiol. Opt. **10**, 186-194 (1990).
5. S. Masuda, S. Takahashi, T. Nose, S. Sato and H. Ito, "Liquid-crystal microlens with a beam-steering function," Appl. Opt. **36**, 4772-4778 (1997).
6. A. F. Naumov, "Modal wavefront correctors," Proc. of P. N. Lebedev Phys. Inst. **217**, 177-182 (1993).
7. A. F. Naumov, G. V. Vdovin, "Multichannel LC-based wavefront corrector with modal influence functions," Opt. Lett. **23**, 1550-1552 (1998).
8. E. G. Abramochkin, A. A. Vasiliev, P. V. Vashurin, L. I. Zhmurova, V. A. Ignatov and A. F. Naumov, "Controlled liquid crystal lens," preprint of P. N. Lebedev Phys. Inst. **194**, 18p. (1988).
9. A. F. Naumov, M. Yu. Loktev, I. R. Guralnik and G. V. Vdovin, "Liquid crystal adaptive lenses with modal control," Opt. Lett. **23**, 992-994 (1998).
10. G. D. Love, J. V. Major and A. Purvis, "Liquid-crystal prisms for tip-tilt adaptive optics," Opt. Lett. **19**, 1170-1172 (1994).
11. F. L. Vladimirov, I. E. Morichev, L. I. Petrova and N. I. Pletneva, "Analog indicator based on liquid crystals," Opto-Mekhanicheskaja Promishlennost **3**, 27-28 (1987).
12. G. D. Love, "Liquid-crystal phase modulator for unpolarized light," Appl. Opt. **32**, 2222-2223 (1993).
13. J. W. Goodman, *Introduction to Fourier Optics* (McGraw-Hill Book Company, New York, 1968).

#9499 - $15.00 US Received March 31, 1999; Revised April 25, 1999

14. A. F. Naumov, M. Yu. Loktev and I. R. Guralnik, "Cylindrical and spherical adaptive liquid crystal lenses," SPIE 3684, pp.18-27 (1998).
15. L. M. Blinov, *Electro-Optical and Magneto-Optical Properties of Liquid Crystals* (Wiley, New York, 1983).
16. A. F. Naumov, M. Yu. Loktev, I. R. Guralnik, S. V. Sheyenkov and G. V. Vdovin, "Modal liquid crystal adaptive lenses," preprint of P. N. Lebedev Phys. Inst. **13**, 28p. (1998).
17. B. R. Frieden (ed.), *The Computer in Optical Research. Methods and Applications* (Springer-Verlag, Berlin, Heidelberg, New York, 1980).

1. Introduction

A large birefringence and a low control voltage distinguish nematic liquid crystals (LCs) from other electro-optical materials. They can be conveniently used as programmable phase modulators for a number of applications. There has been much research on the use of LCs as switchable lenses, where the aim is to produce a LC with an electrically controllable focal length. Most past work has involved the localized addressing of LCs, i.e. the LC cell is divided into separate areas (usually pixels, or zones in the case of a Fresnel lens) [1-3], each of which is controlled by its own separate control voltage. Adaptive lenses with non-uniform LC boundary layers are considered in the review [4]. Microlenses have been produced by a non-uniform electric field caused by hole-patterned electrode structures [5].

LCs respond to the rms value of an applied AC field. This fact has allowed us to develop a new type of electrical addressing, called modal addressing, which allows a continuous variation of the phase profile across a device. We have produced both modal LC wavefront correctors [6,7] and modal LC lenses (MLCLs) [8,9].

MLCLs are simple to make and can produce a smooth change in focal length by controlling the amplitude and frequency of the control voltages. However, these values need to be carefully selected in order to minimize phase aberrations, caused by both the non-ideal distribution of the electrical field across the lens aperture, and the nonlinear electro-optical response of the LC versus the applied field.

In this paper we show how the electrical control parameters can be optimized in order to minimize the lens aberrations, and we present experimental results.

2. Operation principle and numerical optimization of control voltage parameters

The construction of a MLCL is characterized by a high resistance transparent electrode and a low resistance control contact. The contact configuration determinates the type of lens. For spherical lenses we use an annular contact and for a cylindrical lens we use two linear parallel contacts. Although the experimental configuration of MLCLs is similar to other modally addressed LCs [10,11], the principle of operation is different. MLCLs utilize the reactive parameters of the cell, i.e. their electrical response to an AC field. Figure 1 shows a

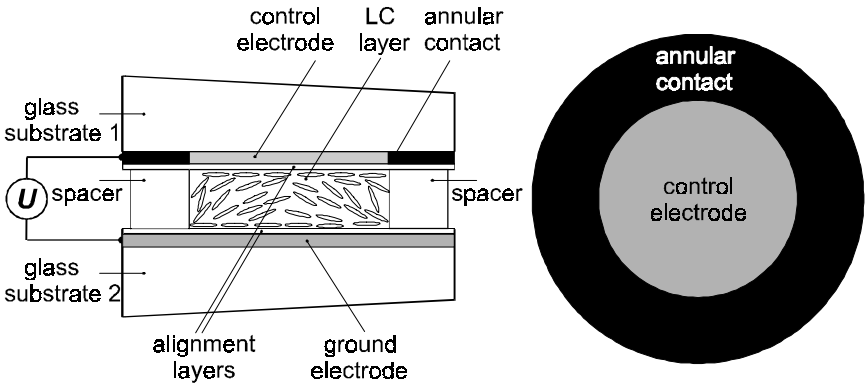

Fig. 1. A spherical modal liquid crystal lens.

#9499 - $15.00 US
Received March 31, 1999; Revised April 25, 1999

spherical MLCL schematically. The control voltage is applied to a low resistance annular electrode around the active area of the lens. The voltage across the lens decreases radially towards the center of the lens, because of the potential divider that is formed by the high resistance control electrode and the capacitance of the LC layer, i.e. its impedance increases radially towards the lens center. This means that the voltage decreases radially towards the center. Conversely, the optical path length of the LC layer increases from the periphery to the aperture center. Note that the incident light must be linearly polarized along the LC's extraordinary axis. To operate with unpolarized light it is necessary to use two identical lenses with mutually orthogonal orientations or to apply the technique described in ref. [12].

The MLCL focal length can be evaluated using Fresnel's approximation [13] as

$$F = \frac{\pi l^2}{(\Delta\Phi_c - \Delta\Phi_e)\lambda}, \tag{1}$$

where $\Delta\Phi_c$ and $\Delta\Phi_e$ are the retardances, measured at the center and edges respectively, l is the MLCL radius, and λ is the wavelength of incident light. The distribution of the rms voltage across the lens is described by Bessel functions [14], and the voltage-retardance dependency $\Delta\Phi(U)$ is approximately an inversion logarithmic function. In general, if a voltage of arbitrary magnitude and phase is applied to the cell, then the resulting phase distribution will be far from parabolic, and the lens aberrations will be significant. However, for a certain relationship between the frequency of the applied voltage and the distributed impedance, the retardance distribution is close to a paraboloid.

The control voltage frequency defines the magnitude of the voltage across the LC, which in turn shapes the electrooptic response. The calculation of the optimal control parameters is computationally intensive because it requires the solution of a second-order partial differential equation, which describes the voltage distribution modulus over the aperture, and contains parametric coefficients connected with the alignment of LC molecules through the integral (see eqs. (1-4) in Ref. [9]). In its turn, the molecular alignment by the electrical field is described by Ericksen-Leslie's equation [15], which is itself a second-order partial differential equation. The numerical solution of this problem is described in Ref. [16]. Figure 2 shows the typical dependencies of the sinusoidal control voltage parameters for a spherical adaptive lens. We used the parameters shown in table 1 for the computation.

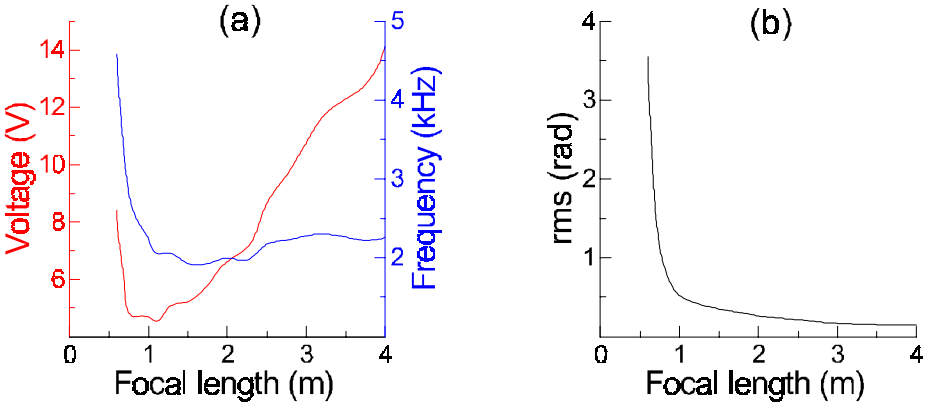

Fig. 2. (a) Theoretical dependence of the optimal control voltages and frequencies versus focal length for a modal liquid crystal lens. (b) Dependence of the rms phase deviation from an ideal parabola versus focal length.

#9499 - $15.00 US
Received March 31, 1999; Revised April 25, 1999

Table 1. MLCL parameters used in compute simulation.

Optimal control	Layer thickness	Aperture size	Pre-tilt angle	Surface resistance	Largest voltage
0.633 μm	25 μm	5 mm	0 degree	31.22 MΩ/sq	10 V

Refraction indexes along ∥ and perpendicularly ⊥ to LC director		Dielectric indexes				Elastic modulus ($dyn\times10^{-7}$)	
		Real part		Imaginary part		Splay	Bend
$N_{\parallel}$	$N_{\perp}$	$\varepsilon_{\parallel}'$	$\varepsilon_{\perp}'$	$\varepsilon_{\parallel}''$	$\varepsilon_{\perp}''$	K_{11}	K_{33}
1.7903	1.5296	9.53	5.1	0.625	0.45	1.2	1.3

From Fig. 2b it can be seen that the value of the rms phase deviation from a parabola increases abruptly for short focal lengths. This increase is explained by noting that in this case the full dynamic range of the LC is being utilized, which is essentially nonlinear. The phase aberrations can be decreased by the introduction of *m* additional harmonics into the control signal. In this case each harmonic will contribute to the phase distribution across the aperture and by optimizing the strength of each harmonic the total rms phase deviation can be minimized. For the control voltage $U_0 \sum_{k=1}^{m} \alpha_k \sin(\omega_k t)$ the computed results obtained by means of a Monte-Carlo method with the descent technique [17] are shown in Fig. 3, and the

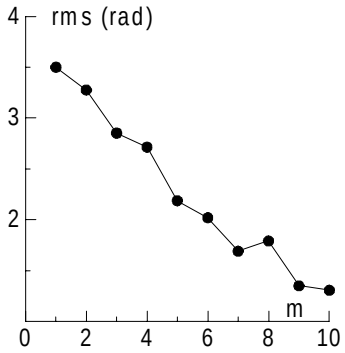

Fig. 3. Dependence of the rms phase deviation from an ideal parabola versus number of harmonic components *m* in the control signal $U_0 \sum_{k=1}^{m} \alpha_k \sin(\omega_k t)$ for $F = 0.6$ m.

harmonic control voltages are better than single harmonic voltages, they are not used in practice for simple adaptive lenses, for a number of reasons. Firstly, it is very difficult to control the lens parameters, such as thickness and electrode resistance, accurately enough. Secondly, the calculation of the control voltage parameters requires significant computing time (for example, the results for only one focal length with 10 harmonics required 10 hours using a Pentium 450 MHz processor). Finally, the improvement is significant only for short focal length lenses. For example, for a focal length of 2 m the optimal 10-harmonic control voltage produces a wavefront with a rms deviation of 0.223 rad, compared with the single-harmonic one of 0.265 rad.

3. Lens calibration

The goal when calibrating the lens is to search for the optimal frequency–voltage pairs for the desired focal length that produce the lens with the minimum rms deviation from a parabola. The MLCL was initially calibrated by placing it between crossed polarizers with its optical axis at 45° to the polarizers' axes, in a collimated He-Ne laser beam ($\lambda = 0.633$ μm), in order to visualize the phase distribution across the lens. The resulting intensity distribution

#9499 - $15.00 US Received March 31, 1999; Revised April 25, 1999

was imaged by an objective lens onto a CCD camera and subsequently processed by a PC. The recovered wavefront was compared with an ideal one, which corresponded to the desired focal length. Using the same descent technique as before we searched for the voltage-frequency values, which produced a phase profile close to parabolic. The experimental apparatus shown in Fig. 4a allowed the calibration of focal lengths from 0.5 m to 1 m. To improve the sensitivity for longer focal lengths (1-4 m) we used a double pass optical set-up, which is shown in Fig. 4b.

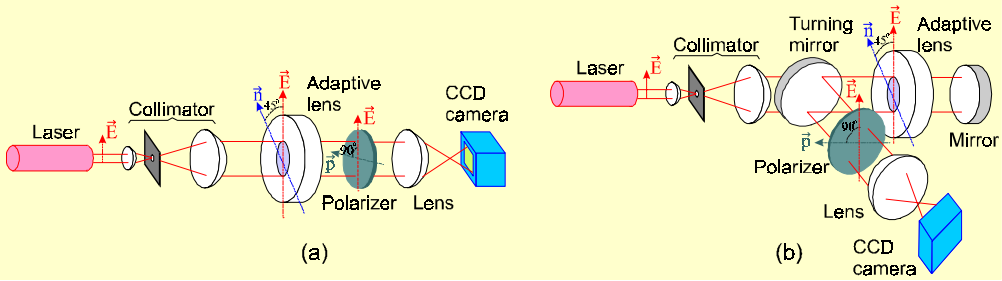

Fig. 4. Optical set-up for calibration of MLCL using (a) single pass and (b) double pass of collimated laser beam through LC layer: $\vec{E}$ is direction of laser beam polarization, $\vec{n}$ is initial alignment of LC molecules, $\vec{p}$ is direction of polarizer orientation.

Because the interference pattern is rotationally symmetrical the wavefront reconstruction was performed using a cross-section. The section center was determined by statistical moments

$$i_0 = \frac{\sum_i \sum_j A_{ij} \cdot i}{\sum_i \sum_j A_{ij}}, \quad j_0 = \frac{\sum_i \sum_j A_{ij} \cdot j}{\sum_i \sum_j A_{ij}}, \tag{2}$$

where i and j are matrix indices of the image $A_{i,j}$. The intensity distribution $B_j = A_{i_0 j}$ in the selected section was smoothed by a convolution with the following Gaussian function in order to remove noise caused by the coherence of the laser beam (speckle noise),

$$\tilde{B}_j = B_j * e^{-\frac{j^2}{\rho^2}}. \tag{3}$$

The Gaussian parameter ρ was adjusted to preserve the signal intensity modulation and reduce coherent noise influence. The local intensity minimum positions were determined by a thresholding method and during this procedure the order number of each minimum with respect to the center was recorded. The position and the order of the minima starting from the center determine the phase distribution across the aperture as $\Delta\Phi_k = -2\pi k/z$, where z is a number of passes of the laser beam through the LC layer and k is the fringe order. A continuous phase distribution was built up by spline interpolation. The phase distribution in the center was approximated by a parabola constructed through the 4 minima nearest to the center points. This phase distribution was compared with the ideal parabolic phase profile and rms deviation was calculated. To calibrate each focal length, approximately 200 steps are required with time delays between them (to allow for the finite LC response time). After calibration for 3–5 focal lengths the approximate dependencies of voltage and frequency on focal distance *U(F)* and *f(F)* are plotted by means of linear interpolation. However the real signal parameters in the intermediate points are then slightly inaccurate. These values were

#9499 - $15.00 US
Received March 31, 1999; Revised April 25, 1999

corrected as follows. The control voltage with the approximate parameters U' and f' for some intermediate focal length F' is applied to the lens. The interferogram obtained in the optical set-up was then recorded and the wavefront was recovered. The real focal length F'', determined from the recovered wavefront, was used as a calibration parameter for the given values U' and f'.

Next we consider the use of bipolar rectangular control voltages. Such voltages can be produced more easily than sinusoidal ones, so we analyzed their use and calibrated their influence on the lens. The calibration results are shown in Fig. 5. It can be seen that the shape of the control voltage becomes less important at longer focal length, and for focal lengths more then 1 m the control voltage shape virtually does not affect the rms. Thus we will use bipolar rectangular control voltages in the next experiment.

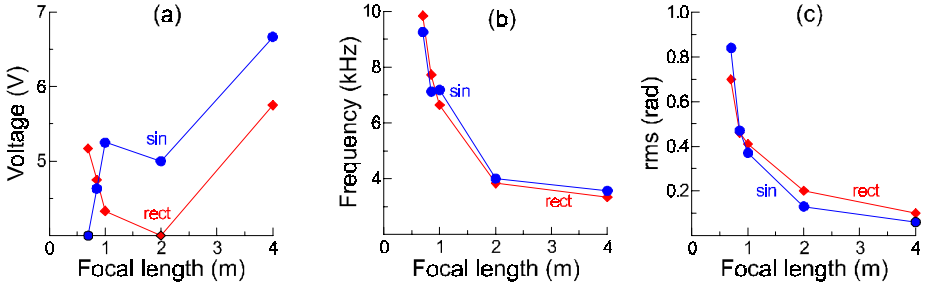

Fig. 5. Calibration by sinusoidal and bipolar rectangular voltage. Optimal voltage (a), frequency (b) and rms dependencies on focal length.

Figure 6 below shows experimental results of four lenses with similar geometric and electrical parameters calibrated using a square wave. It can be seen that the required voltages and phases are not unique for a given focal length. This is caused by the lack of interferometric fringes for the longer focal lengths and the inaccuracy in their position

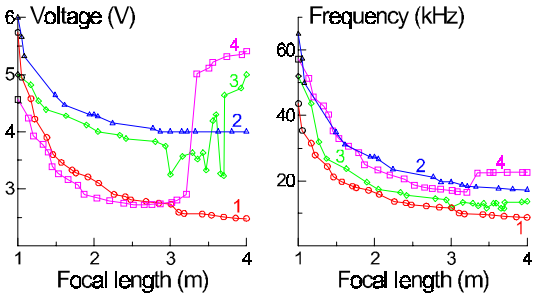

Fig. 6. Optimal control voltage parameters for different experimental samples of MLCL. 1,2,3,4 are for four different lenses.

measurement.

For focal distances greater than 3 m for samples 3 and 4 the optimal voltage and frequency values varied irregularly. Lack of uniqueness in the definition of the control voltage parameters is connected with the possibility of obtaining the same phase distribution for different control voltages, due to the nonlinear dependence of $\Delta\Phi$ on U. For example, to obtain the desired phase profile with depth $\Delta\Phi_0 << \Delta\Phi_{max}$ (see Fig. 7) it is possible to use more than one pair of optimal parameters: voltage - frequency. The voltage applied to the periphery of high-resistance control electrode voltage of U_1 with the frequency f_1 produces the voltage of U_2 at the lens aperture center. The variation of voltages from U_1 to U_2 gives the phase variation equal to $\Delta\Phi_0$ in the experimental error limit. The same result can be obtained

#9499 - $15.00 US
Received March 31, 1999; Revised April 25, 1999

for the voltage of U_3 with the frequency f_2, applied to the angular contact. In this case the distribution of voltages from U_3 at the edge decreases to U_4 at the center and gives the same phase variation in the measure error limit.

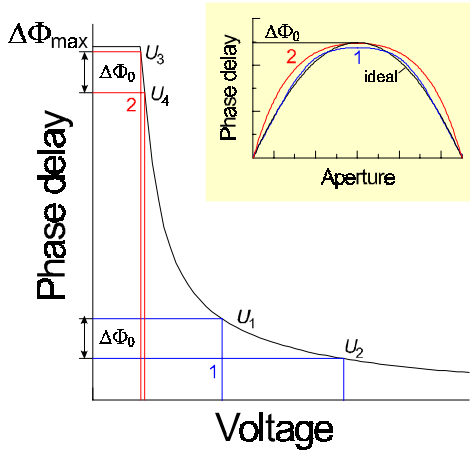

Fig. 7. Demonstration of lack of uniqueness in the definition of the optimal control voltage parameters.

The experimental results of calibration represented in Fig. 8 show that for longer values of the focal length, the region of admissible values of frequencies and voltages assuring a low rms is greater. All results in Fig. 8 are plotted using the same scale window 8 kHz × 6 V. Thus, the lens can be controlled at long focal lengths with a fixed voltage and by varying only the frequency. In this case the maximal possible voltage is preferable. First, a higher voltage produces faster switching times, and secondly, at high voltages the dispersion is reduced. Finally, if the lens has defects in the LC alignment then they are not observed as clearly at higher voltages.

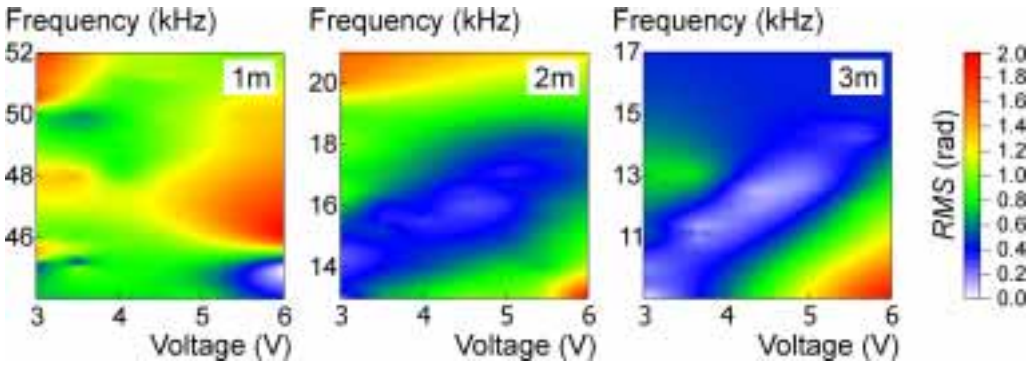

Fig. 8. The alternation of control voltage parameters for different focal lengths.

4. Lens control by variation of control voltage duty cycle.

By using a bipolar rectangular voltage for the lens control there is an additional parameter, which can be easy varied. This is the duty cycle $q = \tau / T$, where τ is the time during which the voltage is positive, and T is the time period. The variation of q leads to a variation of the control voltage spectrum. Figure 9 shows interferograms obtained with the single-pass experimental set-up using different duty cycles of a control voltage with 9 V amplitude and 4 kHz frequency. The values of q are indicated in the upper left corner on inserts. Because the voltage is bipolar the signal spectrum was varied using q from 0.5 to 1, since values from

#9499 - $15.00 US
Received March 31, 1999; Revised April 25, 1999

0 to 0.5 will give identical results. The focal length and the rms phase deviation from a perfect lens are shown on each interferogram.

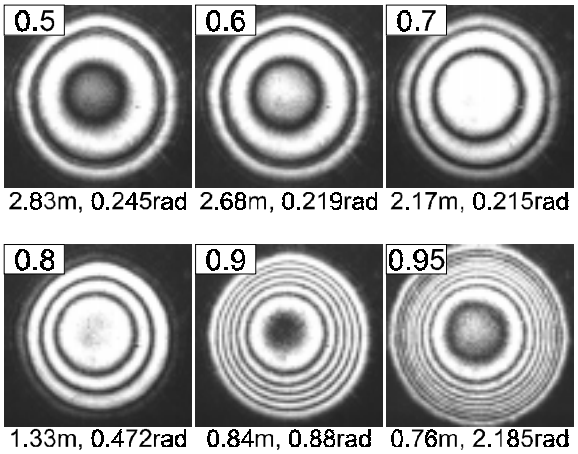

Fig. 9. Interferograms obtained using different duty cycles for bipolar rectangular control voltages with 9 V amplitude and 4 kHz frequency: q is indicated in the top-left corner of each interferogram. The resultant focal length and the rms phase deviation from an ideal parabola are shown on each lower insert.

We did not optimize the q parameter in order to obtain minimal values of the rms phase deviation. The dependence of q on F will be essentially nonlinear. Additionally, the variation of q does not produce the focal length variation over the full range. However the duty cycle control method can be used to minimize lens aberrations further, in a lens that has been calibrated by the usual method for voltages and frequencies at $q = 0.5$.

5. Technical parameters

We have manufactured several LC lenses by using two different methods. The experimental results represented in Figs. 5 and 9 and in the movie, Fig. 10, were obtained by using a MLCL with initial plane alignment. The alignment layers were produced using polyvinyl alcohol (PVA). The surface resistance of the high resistance transparent electrode was 9 MΩ/sq. The other parameters were the same for both kinds of lenses. The ITO low resistance electrode had 50-200 Ω/sq. The thickness of the LC layer in the lenses was 25 μm. We selected a nematic LC with high optical anisotropy and high conductivity. The LC dielectric anisotropy was higher than in the computer simulations, therefore the region of optimal voltages is lower. The aperture diameter was 5 mm. The minimal focal length was 0.5 m.

The results represented in Figs. 6 and 8 were obtained using LC lenses with pre-tilted alignment. In this case the alignment layers were produced using oblique vacuum evaporation of GeO. The pre-tilt angle was approximately 15^{o}. The pre-tilt increased the minimal focal length up to 1 m. The high resistance electrode had the surface resistance of 3-5 MΩ/sq. This required an increase of the optimal control frequencies values. However the pre-tilt and the lower high resistance electrode allow higher LC switching speeds. Investigation of the dynamic characteristics of MLCLs is complex and lies outside the scope of the present work.

In the attachment movie (Fig. 10) the focussing of an image using a MLCL is demonstrated. The object (text) was illuminated by a tungsten lamp. The object frame size was 25×25 mm. It was placed 0.5 m from a camera lens of focal length 80 mm. The MLCL was placed immediately behind the camera lens. It was possible to move the CCD array along the optical axis of the camera lens and to register this displacement. When the MLCL

#9499 - $15.00 US Received March 31, 1999; Revised April 25, 1999

was turned off, the position of the CCD array was adjusted to produce a sharp image. Then the CCD array was moved 2 mm towards the camera lens. This induced defocus can be corrected by applying the appropriate control voltage parameters to the MLCL. We switched on a real-time frame grabber and simultaneously switched off the control voltage. The changing image was then recorded. A similar experiment was performed using the experimental setup in figure 4a. Both movies were combined and synchronized. Between frames we introduced a time delay, in reality the process is faster.

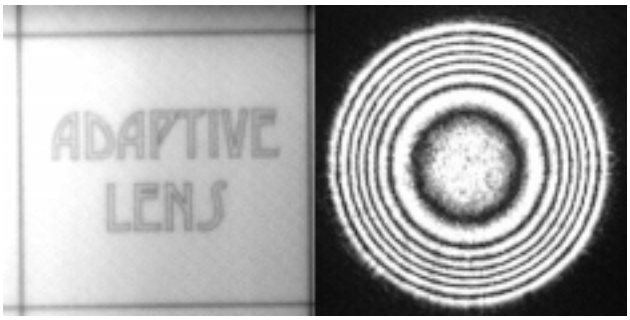

Fig. 10. (507 KB) Correction of defocus by a MLCL (left) and the corresponding interferogram variation (right).

6. Conclusion

In this paper we showed that the imaging performance of a MLCL can be improved by using multi-harmonic control voltages, and we discussed the practicalities of this technique. We experimentally demonstrated the application of bipolar rectangular control voltages and also proposed the additional control of MLCLs by varying the duty cycle. We explained the lack of uniqueness in the specification of the optimal frequency and voltage for large focal lengths. We presented results of a MLCL correcting defocus in an optical system.

Acknowledgements

The authors wish to express their appreciation to Drs. I. Guralnik from Samara State University, Russia for useful discussions, Thu-Lan Kelly for suggestions, which significantly improved this paper and Brett Patterson for his help in preparation of the animation.